JOURNAL OF CATALYSIS **162,** 239–249 (1996)
ARTICLE NO. 0281

Promoting Effect of Pt on Co Mordenite upon the Reducibility and Catalytic Behavior of CO_2 Hydrogenation

Alicia V. Boix, María A. Ulla, and Juan O. Petunchi[1]

Instituto de Investigaciones en Catálisis y Petroquímica, INCAPE (FIQ, UNL-CONICET), Santiago del Estero 2829-3000, Santa Fe, Argentina

Received January 19, 1996; revised April 30, 1996; accepted April 30, 1996

The reducibility of Co and Pt mordenite monometallic and bimetallic samples with different Co/Pt ratios was studied by temperature-programmed reduction. The species formed after reduction were characterized by X-ray diffraction (XRD) and XPS. Co mordenite samples presented a very low reducibility in the 273–823 K range, whereas the Pt monometallic samples were totally reduced in that range with a H_2/Pt ratio = 1. Two well-differentiated reduction zones in the 273–573 K and 573–823 K ranges were observed in these samples, suggesting a Pt^{2+} ions distribution at the exchange sites of the mordenites. A proportion of 70 : 30% for the two zones resulted, independent of the Pt loading. The incorporation of platinum notably increased the Co reducibility. The type and stability of the species formed during the reduction depended on the Co/Pt ratio. In the sample with a lower content of Pt, a catalytic action of the latter prevailed, leading to reduced species formed by a fine dispersion of metallic Co and Pt particles. When the Pt content increased, the formation of $PtCo_xO_y$ species during calcination seemed to be the precursor of the promoting effect. For high contents of Pt (5%), Co/Pt = 0.6, XPS results revealed an important Co–Pt interaction. After sinterization, Pt_3Co particles were clearly observed by XRD. The Pt–Co interaction modified the specific activity and selectivity to CH_4 of the monometallic species in the CO_2 hydrogenation reaction. The samples with a Co/Pt ratio = 5.9 presented a maximum in the methanating activity, thus resulting in a turnover frequency for CH_4 production, $N_{CH_4} = 0.20$ (s^{-1}) at 623 K and 1 atm. This turnover frequency dropped to 0.015 for Co/Pt = 0.6.

1. INTRODUCTION

The interest in CO_2 hydrogenation to obtain hydrocarbons and oxygenated compounds (1, 2) which started in the 1970s has been revived by the need of decreasing the CO_2 levels and their action on the "greenhouse" effect.

Within this framework, the use of bifunctional metal–zeolite catalysts has been lately investigated in order to combine the hydrogenating action of group VIII metals (Fe, Co) with the form selectivity of zeolites (3, 4). One of the hindrances of this system is the difficulty to reduce metallic ions of large electronegative potentials at exchange positions with conventional methods. Thus, Huang and Anderson (5) and Petunchi and Hall (6) found that ion exchanged iron cations in Y zeolite and mordenite could not be reduced to metal with H_2 at 773 K, and Kim and Wood (7) reported that ion exchanged cobalt cations were reduced to a very low degree (less than 5%) under the same conditions, thus resulting in the formation of small zero-valent cobalt clusters (<13 Å). However, Zhang *et al.* (8) showed by temperature-programmed reduction (TPR) that Co^{2+} ions in Y zeolite could not be reduced by H_2 below 900 K. Lu *et al.* (9) analyzed the influence of the different calcination temperatures upon the reducibility of CoY and reported that for calcination temperatures lower than 723 K, they only detected peaks between 800–900 K by TPR, while when calcining at 773 K they did not detect any reduction up to 900 K. An alternative to increase the reducibility of group VIII metals consisted in adding another easily reducible cation, such as Pt or Pd, which not only catalyzed the reduction of the not so easily reducible metal but also interacted with it. Sachtler and Zhang (10) studied different bimetallic systems such as Pt-Cu, Pt-Ni, Pd-Co, and Pd-Cu, in type Y zeolites. Guczi and co-workers also analyzed in detail the Pt-Co systems in NaY (11–13). As far as we know no similar studies have been made on mordenite, except those related to Pt-mordenite (14–16). Recently, Co-mordenite and CoPt mordenite catalysts have been successfully employed in the selective reduction of NO (17).

This work presents a systematic study of the reducibility of Co mordenite (CoM) and the promoting effect of Pt addition. TPR, X-ray diffraction (XRD), and XPS measurements were used to characterize the species formed upon reduction. The activity and selectivity of mono and bimetallic samples toward CO_2 hydrogenation were also investigated.

2. EXPERIMENTAL

2.1. Catalyst Preparation

Monometallic CoM and PtM, and bimetallic CoPtM catalysts were prepared by ion exchange. Na mordenite (Linde

[1] To whom correspondence should be addressed. Fax: 54-42-553727. E-mail: nfisico@fiqus.unl.edu.ar.

0021-9517/96 $18.00

TABLE 1

Metal Content in Catalysts Measured by A.A.

Catalyst[a]	Pt (w%)	Co (w%)	% CEC[b]	Vp (cc/g)[c]	Sg (m^2/g)[d]
$Co_{2.4}M$	—	2.4	42	0.150	350
$Co_{3.0}/SiO_2$	—	3.0	—	—	—
$Pt_{0.5}M$	0.5	—	2.3	0.142	350
$Co_{2.0}Pt_{0.5}M$	0.5	2.0	34	0.140	345
$Pt_{1.0}M$	1.0	—	4.5	0.141	360
$Co_{1.8}Pt_{1.0}M$	1.0	1.8	32	0.143	354
$Pt_{5.0}M$	5.0	—	23	0.142	362
$Co_{0.8}Pt_{5.0}M$	5.0	0.8	32	0.148	335
NaM	—	—	—	0.150	373

[a] The subscript in the nomenclature corresponds to the percentage of weight in metal.

[b] Percentage of cation exchange capacity.

[c] Pore volume (cc/g).

[d] Surface area (BET) (m^2/g) of samples calcined according to the "standard pretreatment."

LZM5, Lot No. 1280-8) of $Na_8[(AlO_2)_8(SiO_2)_{40}] \cdot 24H_2O$ unit cell was used. CoM was prepared using a diluted $Co(NO_3)_2$ solution (0.025 mol/liter) with a zeolite/solution ratio of 2 g/liter.

Co/SiO_2 was prepared by the impregnation method at incipient wetness of SiO_2 (17 m^2/g) with a $Co(NO_3)_2$ solution of adequate concentration, thus obtaining a metal loading of approximately 3% in weight.

PtM with different contents of Pt (5, 1, and 0.5% weight) were obtained from aqueous solutions of $Pt(NH_3)_4(NO_3)_2$ with different concentrations, using a ratio of 2 g of zeolite per 300 ml of solution. In both Co and Pt samples, exchanges of all solids were performed during 24 h at room temperature (r.t.), keeping the pH between 5 and 6. These solids were then filtered, washed, and dried in a stove at 393 K for 12 h.

Bimetallic CoPt mordenite catalysts were obtained by subjecting monometallic Pt mordenite to a second exchange with a $Co(NO_3)_2$ solution following a similar procedure.

All mono and bimetallic solids were calcined after drying in an O_2 flow (30 cm^3 min^{-1}) with a heating rate of 0.5 K min^{-1} up to 623 K, and kept at that temperature for 2 h (18). This pretreatment will be called "standard treatment."

The content of Pt and Co in the solids was determined by atomic absorption and the results are given in Table 1. The samples with different metallic content were designated according to what is expressed in Table 1, where subscripts indicate the percentage in weight of the corresponding metals in the zeolitic samples.

2.2. Temperature-Programmed Reduction

Temperature-programmed experiments were conducted in a flow apparatus equipped with a thermal conductivity detector (TCD); 0.1 g of solid was used which was calcined according to the "standard treatment." After purging with N_2 for 1 h, the sample was cooled in N_2 to room temperature. TPR was performed using 5% of H_2 in Ar (25 cm^3 min^{-1}) with 10 K min^{-1} heating rate, from room temperature to 823 K. After the first TPR, the samples were purged with N_2 for 1 h, reoxidated at 773 K for 2 h in oxygen flow, and cooled to room temperature in N_2 to reach a second TPR (TPR_2). In some cases, the oxidation sequence was afterwards repeated and a third TPR was obtained (TPR_3). The calibration was performed with CuO samples of 0.01 and 0.02 g, the error being $\preceq$10%. The reproducibility of the experiments was $\pm$5% in H_2 consumption and $\pm$5°C in the temperature maxima.

2.3. XRD

Mono and bimetallic catalysts calcined after the "standard treatment" were analyzed by XRD. In addition, the solids mentioned above were studied after being reduced with H_2 at 623 and 773 K, respectively.

X-ray diffraction measurements were taken using CuK_α , radiation at 30 kV and 30 mA, with a Shimadzu diffractometer XD-D1 model using a scanning rate of 1° min^{-1} and values of 2θ from 5 to 50°.

2.4. XPS

The XPS data were obtained in a Shimadzu ESCA-750 spectrometer equipped with a Mg anode (MgK_α = 1253.6 eV). The signal was accumulated and processed using an ESCAPAC 760 computer system. The curve fitting processing was made using Gaussian–Lorentzian component waveforms. In the XPS spectra Si2p was taken as reference, measured for Na mordenite and SiO_2 whose binding energies (B.E.s) were 102.6 and 103.8, respectively.

The samples calcined after the "standard treatment" were degassed through a 5 K min^{-1} heating up to 625 K and kept at that temperature for 2 h. They were afterwards cooled and introduced into the analysis chamber to perform the XPS measurements. Samples were reduced with H_2 in the reaction chamber directly attached to the ESCA spectrometer at the desired temperature.

2.5. H_2 Chemisorption Measurements

After the "standard treatment," solids were reduced with H_2 at 623 K and then evacuated up to 10^{-5} Torr. The experiments were carried out in a conventional volumetric vacuum apparatus.

The metal surface area was then determined by H_2 chemisorption at 298 K. The total hydrogen adsorption uptake was determined as a function of pressure and the linear portion of the isotherm extrapolated to zero pressure to obtain the chemisorbed amount.

2.6. $CO_2 + H_2$ Reaction

The CO_2 hydrogenation activity was determined using 0.1 to 0.5 g of catalyst in a quartz microreactor operated at atmospheric pressure. The H_2/CO_2 ratio was 4 and the temperature reaction was 623 K.

Solids were calcined following the "standard treatment" and subsequently reduced with flowing H_2 during 1 h at 623 K before the reaction. The CO_2 conversion and the selectivity to methane were evaluated as a function of the residence time variation, calculating the initial rate of CO_2 conversion and the selectivity to methane. In every case, the reaction products were CO, CH_4, and traces of C_{2+}.

All reactant and product gas concentrations were chromatographically measured using thermal conductivity with a Porapak Q column, 39 in. long and 1/8 in. i.d., and flame ionization detectors.

3. RESULTS

3.1. Monometallic Catalysts TPR

The TPR profiles for $Co_{2.4}M$ are shown in Figs. 1a and a′. In the first TPR (Fig. 1a), after the "standard treatment" the main peak appeared at 600 K, with a small shoulder at approximately 650 K. Three smaller ones were observed at 710, 773, and 823 K. The second reduction (TPR_2, Fig. 1a′) after reoxidation at 773 K, was similar to the first one. However, two peaks clearly appeared at 580 and 650 K, and only one at higher temperatures. The degree of cobalt reduction did not vary significantly although the reoxidation was performed at a higher temperature (Table 2).

The reduction of $Co_{3.0}/SiO_2$ is presented in Figs. 1b and b′. The consumed H_2 mol/cobalt mol ratio resulted 1.1 for both reductions.

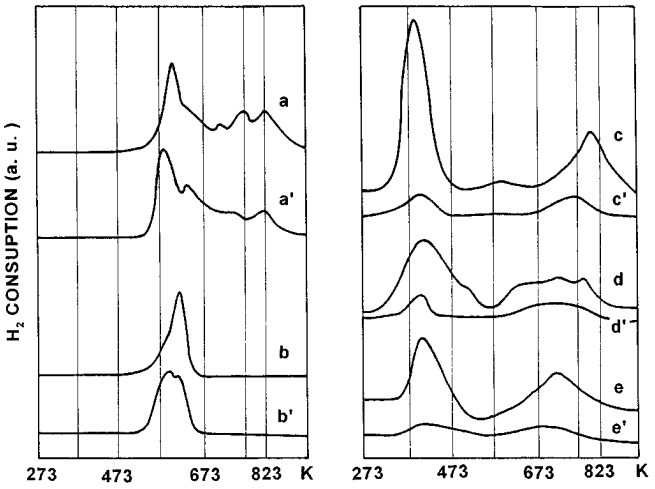

FIG. 1. TPR of monometallic catalysts: $CO_{2.4}M$ (a, a′), $Co_{3.0}/SiO_2$ (b, b′), $Pt_{5.0}M$ (c, c′), $Pt_{1.0}M$ (d, d′), and $Pt_{0.5}M$ (e. e′). The first TPR was run after calcination at 623 K (a, b, c, d, e) and the second TPR was run after reoxidation at 773 K (a′, b′, c′, d′, e′).

The monometallic Pt solids presented similar reduction thermograms for different contents of platinum (5, 1, 0.5%w) (Figs. 1c–e). In Table 2, it can be seen that for $Pt_{1.0}M$ (Fig. 1d) and $Pt_{0.5}M$ (Fig. 1e), after calcining at 623 K, the main peak appeared at approximately 420 K, whereas in $Pt_{5.0}M$ (Fig. 1c), it did so at a slightly lower temperature. In all samples a second peak was observed at temperatures higher than 700 K, the reduction being completed at 823 K. The H_2 consumption calculated from each TPR curve indicated that about one hydrogen molecule was consumed per Pt ion as shown in Table 2. This implies that most Pt remained in a divalent state after calcination at 623 K. Despite the slightly different shape of the thermograms according to the Pt content, the H_2/Pt ratio was quite the same in both the low (273/573 K) and the high (573/823 K) temperature ranges, regardless of the Pt loading. In the second reduction (TPR_2) after reoxidating the solids at 773 K, the hydrogen consumption notably decreased (Table 2) but the position of the peaks was similar to that in TPR_1 (Figs. 1c′, d′, and e′).

3.2. Bimetallic Catalysts TPR

The TPR profiles of the bimetallic solids calcined at 623 K are shown in Figs. 2a–c. CoM was also included (Fig. 2d) for comparison purposes. In all the CoPtM samples, two different reduction zones were observed, one at low temperatures from 273 to 573 K, and the other one at higher temperatures from 573 to 823 K.

The incorporation of 0.5% of Pt notably increased the reducibility of Co in the zeolitic matrix. Note that the H_2 consumption of the high temperature zone was considerably higher than that of the low temperature zone (Table 2). The reduction maxima were present at 473 and 800 K, shifted 50 K to higher temperatures with respect to the Pt monometallic sample (Fig. 1c). The species formed in the first reduction were partially reoxidated in oxygen flow at 773 K. The TPR performed over the reoxidated samples revealed an unfolding of the reduction peaks in the two temperature regions, the signals being broader. In the subsequent cycles of oxidation–reduction the sample had a reversible behavior (Table 2).

When the Pt content of the samples was doubled, a somehow different behavior was observed. In effect, the sample presented two reduction zones in the same range of temperature as before, but the H_2 consumption was lower. Note that by assuming that in both samples all the Pt had been reduced in the $Co_{1.8}Pt_{1.0}M$ only 13% of the cobalt was reduced against almost 50% in the $Co_{2.0}Pt_{0.5}M$ sample. Another difference that should be remarked is that in the $Co_{1.8}Pt_{1.0}M$ sample, the H_2 consumption in the high temperature zone was significantly lower. When the solid was treated in O_2 at 773 K the reoxidation was practically total, a noticeable reproducibility being observed in the successive TPRs.

To dilucidate the effect of the increase of the Pt content on Co reducibility a sample with 5% of Pt was prepared,

TABLE 2

Reducibility of Co_xPt_y Mordenite

Catalysts[e]	T (K)[a]		T_{max}[b]		μ moles H_2[c]		$H_2/(Pt+Co)$[d]	
					273–573	573–823	273–573	573–823
$Co_{2.4}M$	623	600	773	823	0.7	0.6	0.017	0.014
	773	580	650	823	0.9	0.6	0.021	0.014
$Pt_{5.0}M$	623	385		820	18	10	0.74	0.36
	773	410		773	2	2	0.08	0.07
$Co_{0.8}Pt_{5.0}M$	623	398		823	42	13	1.04	0.32
	773	363	609	773	28	15	0.69	0.37
Co/Pt = 0.6[f]	773	342	608	773	18	14	0.43	0.33
$Pt_{1.0}M$	623	418	750	800	3.55	1.78	0.69	0.35
	773	405		803	0.51	0.77	0.10	0.15
$Co_{1.8}Pt_{1.0}M$	623	434	649	773	6.75	2.44	0.19	0.07
	773	455	673	788	5.95	1.88	0.16	0.05
Co/Pt = 5.9	773	455	694	803	6.10	3.37	0.17	0.10
$Pt_{0.5}M$	623	420		723	1.9	0.8	0.74	0.31
	773	420		723	0.2	0.3	0.08	0.12
$Co_{2.0}Pt_{0.5}M$	623	473		800	7.5	12	0.21	0.33
	773	350	523	800	5.3	7.8	0.14	0.21
Co/Pt = 13.3	773	473		773	4.9	7.4	0.13	0.20

[a] Before the first TPR, calcination was performed after the "standard treatment" at 623 K, and for the following ones (TPR_2, TPR_3) oxidation took place at 773 K.

[b] Maximum temperature in TPR peaks.

[c] H_2 consumption in TPR (μ moles) per 0, 1 g.

[d] The range considered in the evaluation of H_2 consumption was (273–573) and (573–823) K, except for CoM where the ranges were (273–673) and (673–823) K.

[e] The subscript in the nomenclature indicates the percentage in weight of metal in the solid.

[f] Molar ratio.

the Co/Pt ratio resulting 0.6 against 5.9 and 13.3 of the $Co_{1.8}Pt_{1.0}M$ and $Co_{2.0}Pt_{0.5}M$ samples, respectively.

In $Co_{0.8}Pt_{5.0}M$ TPR_1 (Fig. 2a, Table 2) the reduction maxima occurred at 398 and 823 K, slightly displaced towards higher temperatures with respect to $Pt_{5.0}M$ but at lower temperatures than the first maximum of $Co_{2.4}M$ (600 K). The molar ratio of the hydrogen consumption with respect to cobalt plus platinum ($H_2/(Co + Pt)$) for the whole range under study was 1.36 (Table 2); this would indicate that platinum and/or cobalt have an average valence higher than (+2). In this sample a higher H_2 consumption was also observed in the low temperature zone.

When $Co_{0.8}Pt_{5.0}M$ was reoxidated at 773 K and then a second TPR was performed, the maxima were displaced towards lower temperatures (Fig. 2a′) and a decrease of the H_2 consumption with respect to TPR_1 was observed in the first peak (T < 573 K), whereas for temperatures higher than 573 K, it remained constant. The thermogram shape in the 573–823 K range changed with respect to the first one. In fact, a less definite peak appears after the first TPR and the resulting profile resembled the one obtained with Co mordenite (compare Figs. 2a′ and d′).

3.3. XRD

The monometallic catalysts Pt_xM and $Co_{2.4}M$ and the bimetallic Co_xPt_yM were given the "standard pretreatment" prior to the study by XRD. The diffractograms obtained were coincident with those of the original Na mordenite. This indicates a conservation of crystallinity. Additional data on surface area measurements and pore volume confirm that there is no break of the support structure during the calcination treatment (Table 1). No signals corresponding to platinum or cobalt species were observed in the spectra of the PtM and CoM monometallic solids, reduced with H_2 at 623 and 773 K, which could indicate that the particles formed have a smaller size than the detection limit of the instrument (40 Å, approximately). In Co/SiO_2 reduced at 773 K, the main signal ($2\theta = 44.1^\circ$) belonging to metallic cobalt was observed.

The spectra obtained for the bimetallic solids are shown in Fig. 3. Only for the $Co_{0.8}Pt_{5.0}M$ catalyst reduced at 773 K (Fig. 3) is a well-defined peak observed whose maximum is located at $2\theta = 40.5^\circ$. It would correspond to $CoPt_3$ bimetallic clusters, whose main peak coincides with this value (19).

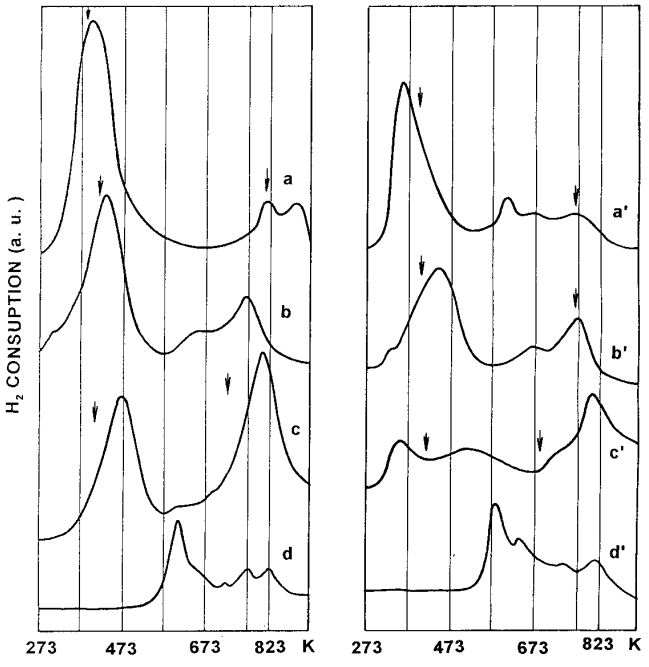

FIG. 2. TPR of bimetallic catalysts: $Co_{0.8}Pt_{5.0}M$ (a, a′), $Co_{1.8}Pt_{1.0}M$ (b, b′), $Co_{2.0}Pt_{0.5}M$ (c, c′), and $Co_{2.4}M$ (d, d′). The first TPR was run after calcination at 623 K (a, b, c, d) and the second TPR was run after reoxidation at 773 K (a′, b′, c′, d′). The arrow shows the location of TPR maxima of PtM.

Applying Scherrer's equation to this peak, it is possible to estimate a crystal size of approximately 50 Å.

These results would indicate that the reduction treatment at 773 K provokes the sinterization of small bimetallic particles ($CoPt_3$) and, as a consequence, they become visible to XRD.

3.4. XPS

The B.E.s of the different solids are presented in Table 3. In $Co_{2.4}M$, the value of B.E. obtained for $Co2p_{3/2}$ corresponded to 783.4 eV, which was not modified after a prolonged reduction (4 h) at 700 K. This signal was assigned to ions of Co^{2+} located at exchange positions within the zeolitic structure, in agreement with other authors for Co^{2+} ion exchanged in ZSM5 (20) and Y-zeolite (21). It must be noted that there exists a difference of approximately 2 eV with respect to the binding energy measured for the cobalt oxide supported in silica (Co/SiO_2).

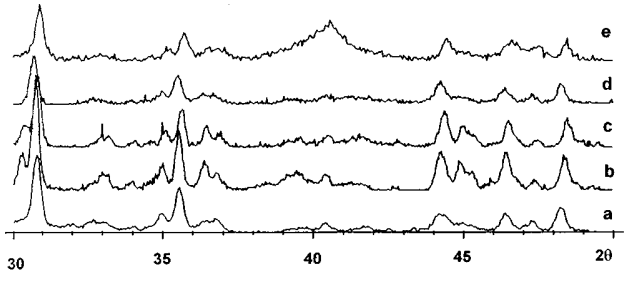

FIG. 3. XRD profiles of: Na mordenite (a); $Co_{1.8}Pt_{1.0}M$ reduced at 773 K (b); and $Co_{0.8}Pt_{5.0}M$ calcined at 623 K (c), reduced at 623 K (d), and 773 K (e).

TABLE 3

XPS Results Data of Co_xPt_y Mordenite

		Binding energy (eV)[a]				
		$Co2p_{3/2}$			$Pt4f_{7/2}$	
Catalyst	Treatment	Shake-up	Co^{2+}	Co°	Pt^{2+}	Pt°
Co/SiO_2	Cal. 673 K	—	781.5	—	—	—
	Red. 653 K	784.6	—	778.2	—	—
$Co_{2.4}M$	Cal. 673 K	788.6	783.4	—	—	—
	Red. 700 K	788.8	783.3	—	—	—
$Co_{0.8}Pt_{5.0}M$	Cal. 673 K	788.7	783.3	—	73.3	71.9
	Red. 653 K	788.5	783.2	778.7	73.1	71.9
$Co_{1.8}Pt_{1.0}M$	Cal. 673 K	788.4	783.1	—	—	71.7
	Red. 653 K	788.7	783.3	778.3	—	71.6

[a] The binding energy values are referred to Si2p (102.0 eV), except in SiO_2, where the reference was Si2p (103.8 eV).

The binding energy of the $Pt4f_{7/2}$ measured in calcined $Pt_{5.0}M$ (71.8 eV) was slightly modified after reduction with H_2 (71.6 eV). These values are similar to those observed by Vedrine *et al.* (22) for Pt° highly dispersed in Y zeolite. In the samples with a lesser content of platinum, $Pt_{1.0}M$, the B.E. was similar to $Pt_{5.0}M$.

In an additional experiment, it was observed that in noncalcined $Pt_{5.0}M$, as the evacuation temperature in high vacuum (10^{-8} Torr) increased, the decomposition of the Pt tetraammine ion provoked the reduction of the ion at surface level.

In $Co_{0.8}Pt_{5.0}M$, the binding energy of Pt^{2+} and Pt° was observed, not only in the calcined solid, but also in the reduced one. Instead, in the solid with a lower content of platinum, $Co_{0.8}Pt_{1.0}M$, only metallic platinum was observed. It should be remarked that the signal of Pt4f overlaps that of Al2p; consequently, in the solids with a lower content of platinum the fitting with Gaussian curves involves a greater error in the determination of the binding energies.

The binding energies of $Co2p_{3/2}$ in the calcined bimetallic solids were similar to those of $Co_{2.4}M$, but after the *in situ* reduction treatment the presence of metallic Co was detected.

3.5. $CO_2 + H_2$ Reaction

CO_2 hydrogenation was used as a reaction test in mono and bimetallic catalysts previously reduced with H_2 at 623 K. The results obtained are presented in Tables 4 and 5 and Fig. 4. In all the samples under study the main reaction products were CH_4 and CO, a selectivity to C_{2+} products

TABLE 4

$H_2 + CO_2$ Reaction

Catalyst	D[a]	R_{CO_2}[b]	N_{CO_2} (s^{-1})[c]	$N_{CH_4} \times 10^3$ (s^{-1})[d]
$Co_{2.4}M$	0.88	7.5×10^{-4}	0.04	4
$Pt_{5.0}M$	0.80	0.04	0.05	15
$Co_{0.8}Pt_{5.0}M$	0.50	0.16	0.16	0.2
$Pt_{1.0}M$	0.80	0.07	0.09	1.4
$Co_{1.8}Pt_{1.0}M$	0.81	0.48	2.53	202
$Pt_{0.5}M$	0.86	0.05	0.07	0.7
$Co_{2.0}Pt_{0.5}M$	0.79	0.08	0.38	106
$Co_{3.0}/SiO_2$	0.30	0.06	0.20	22

[a] Dispersion, considering H : metal = 1 : 1. The samples were reduced in H_2 flow at 623 K prior to the chemisorption measurements of H_2 at room temperature.

[b] Initial conversion rate (mol CO_2 converted/total mol(Co + Pt)s.).

[c] Turnover frequency for CO_2 conversion (to CH_4, CO, and C_{2+}) (mol reacted/reduced metal sites · s) at 623 K, 1 atm, and $H_2/CO_2 = 4$.

[d] Turnover frequency for CH_4 production mol formed/reduced metal sites · s).

lower than 0.1% being observed, except for $Co_{2.4}M$, where it resulted in 4%.

The specific activity of CoM was much lower than Co/SiO_2. Note that the metallic cobalt is highly dispersed in the mordenite structure.

In the PtM monometallic samples the values of the specific activity, at constant dispersion, were independent of the platinum content. However, the turnover frequency of methane production increased with the platinum content.

TABLE 5

Reactor Composition Outlet as a Function of Space Velocity[a]

Catalyst	GHSV (h^{-1})	X_{CO_2} (%)	$Y_{CO} \times 10^2$	$Y_{CH_4} \times 10^2$
$Co_{0.8}Pt_{5.0}M$	2535	24	4.8	0.048
	1586	27	5.3	0.092
	793	31	6.0	0.18
$Pt_{5.0}M$	1800	28	1.7	3.9
	1028	30	1.6	4.4
	800	34	1.4	5.4
$Co_{1.8}Pt_{1.0}M$	5143	23	3.4	3.0
	2571	34	3.7	5.0
	1333	47	4.1	5.8
$Pt_{1.0}M$	792	29	5.0	1.0
$Co_{2.0}Pt_{0.5}M$	3000	30	2.7	3.2
	1636	37	2.2	5.2
	1091	41	2.0	6.2
$Pt_{0.5}M$	792	20	3.8	0.2
[b]		34.5	7.0	—
[c]		84	~0	30

[a] Reaction conditions: 623 K, 1 atm, and $H_2/CO_2 = 4$.

[b] Thermodynamic equilibrium composition assuming $CO_2 + H_2 \rightleftarrows CO + H_2O$.

[c] Thermodynamic equilibrium composition assuming: $CO_2 + H_2 \rightleftarrows CO + H_2O$; $CO_2 + 4H_2 \rightleftarrows CH_4 + H_2O$; $CO + 3H_2 \rightleftarrows CH_4 + H_2O$.

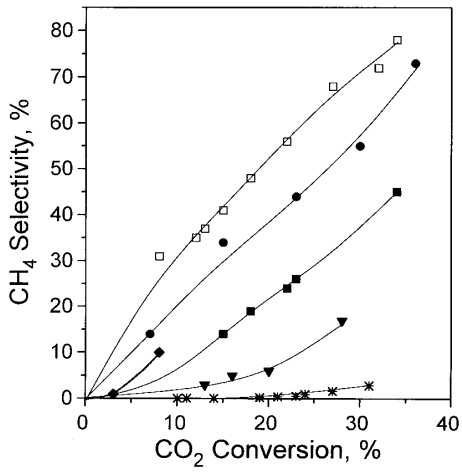

FIG. 4. S_{CH_4} vs. X_{Co_2} of reduced catalysts at 623 K: $Pt_{5.0}M$ (□); $Co_{2.0}Pt_{0.5}M$ (●); $Co_{1.8}Pt_{1.0}M$ (■); $Pt_{1.0}M$ and $Pt_{0.5}M$ (▼), $Co_{2.4}M$ (◆); $Co_{0.8}Pt_{5.0}M$ (∗). Reaction conditions: 623 K, 1 atm, $H_2/CO_2 = 4$.

The behavior of bimetallic catalysts was very different from that observed in monometallic ones. For the solid with a higher content of platinum, $Co_{0.8}Pt_{5.0}M$, where the formation of $CoPt_3$ clusters could be observed, the specific activity of CO_2 conversion was higher than that of all the monometallic ones. However, the CH_4 production was the lowest, thus suggesting that the alloy formed is nonselective.

In the solids with lower platinum content, $Co_{1.8}Pt_{1.0}M$ and $Co_{2.0}Pt_{0.5}M$, a strong increase in the methanating activity was observed. For all mono and bimetallic solids (Fig. 4) the selectivity to methane increased with conversion, which would indicate the same reaction path in all the solids.

4. DISCUSSION

The results obtained in this work show that the incorporation of Pt to the Co mordenite samples substantially increased the Co reducibility in the zeolitic matrix and modified its catalytic properties in the CO_2 hydrogenation reaction.

In order to analyze such influence, it is necessary to discuss beforehand the results obtained in CoM and PtM monometallic solids and then to correlate them with the bimetallic samples behavior. We will then relate their catalytic activity in CO_2 hydrogenation with the type of species formed after reduction of the samples.

Co Mordenite

Cobalt exchanged in Na mordenite ($Co_{2.4}M$) showed a very low degree of reduction, less than 5% (Table 2) in the range of temperatures analyzed. Similar results were reported by other authors in CoY, who studied isothermal reductions with pure H_2 at 773 K (7).

In the thermograms corresponding to $Co_{2.4}M$ it should be observed that a fraction of the cobalt was reduced at temperatures lower than 673 K. In view of the TPRs of Co/SiO_2 (Figs. 1b and b′), this peak at low temperatures could be assigned to the reduction of oxidized species. The reduction range and the characteristics of this peak agree with what is reported in the literature for supported and nonsupported cobalt oxides. (23, 24). The presence of cobalt oxides could be due to the formation of hydroxide species at low concentrations during the ionic exchange. This was proposed by Schoonheydt *et al.* (25), who studied the exchange of Cu^{2+} and Ni^{2+} in *Y* and *X* zeolites (at pH 5–7), suggesting the formation of polynuclear complexes of the $M_x(OH)_y^{2x-y}$ type in the solution, which were then exchanged and/or precipitated in the solids.

Through XPS only the $Co2p_{3/2}$ signal was observed corresponding to Co^{2+} ions at exchange positions (Table 3). No Co^{2+} signal belonging to the oxide could be detected since it represents only approximately 1.7% of all the cobalt (Table 2). The reduction of the exchanged Co yielded three peaks between 723 and 823 K. Comparable results were reported by Lu *et al.* (9) for CoY. They showed that reduction started only at 773 K, presenting two maxima at 803 and 843 K. These authors attributed this behavior to different Co^{2+} in the small cages of the Y-zeolites structure. The mordenite structure does not have such small cages but it has exchanged sites of different stability and location. In fact, Mortier (26), in his studies of Ca mordenite, determined, six different exchanged sites for Ca^{2+} ions, viz. sites I in the center of the small channel; sites II, III, and IV in the interconnecting channels; and sites VI in the main channel. The reducibility of the cations will depend on the site where they are located, since they have different amounts of coordinated oxygens. In the case of Ca^{2+}, Mortier reported the following sequence of population (stability) of the sites for dehydrated samples at 623 K: I > VI > IV > III, the stability of sites IV and III being reversed at elevated temperatures.

Taking into account that Co^{2+} and Ca^{2+} are both bipositive and that they have similar radii, it can be assumed that Co^{2+} ions occupy sites similar to those of Ca^{2+}.

An increase in the reoxidation temperature (773 K) with respect to calcination (623 K) did not bring about appreciable changes in the corresponding thermograms, indicating a reversible process in the oxide-reduction stages.

Pt Mordenite

All monometallic Pt-containing samples presented two reduction regions (Fig. 1), one at low temperatures (lower than 573 K) and another at temperatures higher than 573 K. The H_2 consumption per Pt atom in each region was comparable, independently of the Pt loading of the solid. These results somehow differ in certain aspects from those published by Lerner *et al.* (14), who studied the reducibility of PtNa mordenite and PtH mordenite with different Pt loadings. These authors found that in all cases reduction was completed at 573 K. The different reducibility zones found in samples used in this study could be attributed either to the formation during calcination of different Pt species, viz. PtO, PtO_2, and Pt^{2+} located at exchanged sites, or exclusively to Pt^{2+} ions exchanged at the sites with different coordinations previously described.

In the calcination of ammine ligand precursors even at low heating rate and high O_2 flow, some autoreduction could occur. The Pt clusters thus formed could react with O_2 producing PtO particles and possibly also some PtO_2, which by reacting with the H^+ of the zeolites would partially regenerate Pt^{2+} (27). From the TPR results (Table 2) we could conclude that PtO_2 was not formed. In fact, for all the Pt monometallic samples the H_2/Pt ratios were close to one.

Ostgard *et al.* (27) in their studies of Pt/KL zeolites, reported that PtO particles were reduced at 284 K, while Park *et al.* (28) concluded that such species formed in the supercages of the *Y*-zeolites were reduced at about 323 K. Taking these results into account, and from the TPR profile shown in Figs. 1c, d, e and Table 2, it seems likely that in the Pt monometallic samples PtO particles were not formed. Consequently, in the PtNa mordenites calcined at 623 K there would be a distribution of Pt^{2+} ions at exchanged sites. Taking into account the H_2 consumption of the low and high temperature reduction regions (Table 2), 70% of the platinum ions were located at easily reducible sites, probably sites I and VI, as suggested by Lerner *et al.* (14). The rest of the Pt^{2+} were located at such sites so that if platinum ions were to be reduced, they would probably require the catalytic action of Pt° which was formed at low temperatures. These sites could be of type III, located in the interconnecting channel. The Pt° particles size estimated from H_2 chemisorption (Table 4) suggested that agglomerates of Pt atoms smaller than 20Å in diameter were formed after reduction of the samples at 623 K. However, when the samples were reduced up to 823 K and kept at this temperature for 30 min the sinterization of Pt° would occur as were suggested by TPR_2 (Figs. 1c′, d′, e′). This could be explained by the model proposed by McCabe *et al.* (29) for the reoxidation of Pt supported on SiO_2 and Al_2O_3. They established that the oxidizability of platinum decreases with the particle size increases ranging from essentially complete oxidation for particles with radii smaller than 7.5 Å to less than 10% for particles bigger than 30 Å.

CoPt Mordenite

From the thermograms obtained for bimetallic solids, it is clear that their behavior does not correspond to the sum of each monometallic one: CoM plus PtM; instead, there is a promoting effect of platinum over the reducibility of cobalt.

Despite the different zeolite structure, our results are in general agreement with the ones reported by Lu *et al.* (9)

for PtCoY zeolite. These authors suggested two possible ways for the mechanism of the platinum promoting effect. First, topographically isolated cobalt ions or oxides can be reduced by the hydrogen atoms generated by the platinum which has been reduced at the commencement of reduction; second, cobalt is reduced in $PtCo_xO_y$ oxides that may be formed during calcination. In CoPt mordenites both mechanisms seem possible, depending on the prevalence of one with respect to the other in the Co/Pt ratio of the sample.

In the sample with a lesser platinum content, $Co_{2.0}Pt_{0.5}M$, the increase in the reducibility of cobalt at low temperatures could be attributed to the formation of such types of oxides located in the main channel of the mordenite structure, whereas the reduction at high temperatures would correspond to the catalytic action of platinum upon the nearby Co^{2+} cations.

The bimetallic species resulting from the reduction of $PtCo_xO_y$ were segregated after reoxidation at 773 K. Probably after reduction clusters of highly dispersed Pt° and Co° were obtained which when being reoxidated could form two phases: Pt oxide and Co oxide, probably supported on the external surface of the zeolite (Fig. 2c′).

The thermogram obtained in the second TPR (Fig. 2c′) suggested that the Co° particles formed after reduction at temperatures higher than 573 K were reoxidated to Co^{2+} when samples were treated in O_2 at 773 K. The decrease in H_2 consumption (Table 2) could be a consequence of a migration of Co^{2+} ions to more hidden sites which avoid a close contact with Pt° particles.

The TPR of the $Co_{1.8}Pt_{1.0}M$ sample would indicate that an increase of Pt results in a noticeable decrease of the catalytic action of Pt in the reducibility of Co^{2+} (Fig. 2b and Table 2). The bimetallic oxide particles formed during calcination would appear now more responsible for the Pt promoting action upon Co reducibility. The reduction of these particles leads to species that do not segregate during the successive cycles of oxide reduction.

The results obtained by XPS studies (Table 3) do not supply additional evidence of the possible formation of bimetallic particles either after calcination or reduction at 653 K. In effect, no shift of the binding energy of the $Co2p_{3/2}$ of Co^{2+} and Co° was observed compared to CoM and Co/SiO_2, respectively, probably due to the low number of particles (Table 2). Pt° particles at surface level were the only platinum species observed both in the oxidated and in the reduced samples. In no case were the particles formed higher than 50 Å, according to the XRD results (Fig. 3).

In the solid with a high Pt/Co ratio, $Co_{0.8}Pt_{5.0}M$, two reduction zones were also distinguishable but now, at low temperatures, almost all the ions were simultaneously reduced ($H_2/(Pt + Co) = 1.04$). The fact that along the whole range the H_2 consumed per (Co + Pt) mol was much higher than the unit (Table 2) would indicate that during calcination ionic species with an oxidation state higher than (+2) were formed (for example, PtO_2). Note that the catalytic effect of Pt in the cobalt reduction at high temperatures appears again in this sample (Fig. 2a and Table 2). This could suggest that the particle reduction of bimetallic oxides, which would have a different stoichiometry from that of $Co_{1.8}Pt_{1.0}M$, leads to bimetallic particles rich in Pt on the surface or to the segregation of bimetallic particles during their formation as found for the $CoPt_3$ alloy. Here a sandwich structure is formed with the outermost atomic layer being essentially pure platinum and the second layer being enriched in cobalt (30).

Different from what occurred with the $Co_{1.8}Pt_{1.0}M$ samples, XPS studies also point out the possible existence of bimetallic compounds. In effect, results show the interaction between both ions in the bimetallic solid. The B.E. of $Pt4f_{7/2}$ has a positive shift to $Pt_{5.0}M$. The binding energy of Pt° in the bimetallic solid (71.9 eV), reduced at 653 K, presented a shift towards more positive values with respect to $Pt_{5.0}M$ (71.6 eV). Besides, in the reduced bimetallic samples signals corresponding to oxidated species can be observed, which could be attributed to Pt^{2+} and which were not detected in the monometallic $Pt_{5.0}M$. The B.E. of $Co2p_{3/2}$ in $Co_{0.8}Pt_{5.0}M$ reduced at 653 K indicates the presence of Co° species, but with a positive shift of approximately 0.5 eV with respect to Co/SiO_2.

Similar shifts in the B.E. of both ions were observed by Zsoldos *et al*. (12) in PtCoY. A similar positive B.E. shift for $Co2p_{3/2}$ was observed in $CoPt_3$ intermetallics (30). The XRD results for $Co_{0.8}Pt_{5.0}M$ reduced at 773 K confirm the presence of the $CoPt_3$ bimetallic species. This bimetallic compound could also be formed after reduction of the mixed oxides at 623 K but it became visible to XRD only after sinterization of the metallic particles due to the H_2 treatment at 773 K. These bimetallic particles became unstable upon treatment in oxygen at 773 K. A partial segregation of Co^{2+} particles was observed, part of which would migrate to exchange positions, whereas others would form cobalt oxide supported on the mordenite surface (compare the TPR profiles a, a′, and d′ in Fig. 2). The same type of behavior was reported by Guczi *et al*. (13) for Pt-Co bimetallic particles in Na-Y zeolites. They suggested a decomposition mechanism where the Co^{2+} ions formed segregated to the outermost surface of the metal particles, detached from the surface, and migrated to the sodalite and hexagonal cages. They did not observe the formation of CoO particles, probably due to the low heating rate (0.5 K/min) used in their experiment. The possible formation of adducts between protons and the zero oxidation state of Pt°, similar to the one discovered by Sachtler and co-workers (10) in PdY samples, as well as the probable effect of this interaction on the CoPt bimetallic composition cannot be disregarded. Nevertheless, it was not possible to detect such adducts under the conditions in which this study was carried out.

CO_2 Hydrogenation Reaction

Two purposes generated the study of CO_2 hydrogenation on the mono and bimetallic samples of Co and Pt in mordenite: the feasibility of using such reaction in order to obtain additional information on the characteristics of the species formed after reduction and the possible availability of active and selective solids in the said reaction.

Before performing an analysis of the results obtained in Co-containing catalysts, it is adequate to remark on certain aspects of the catalytic behavior of that metal in the hydrogenation of carbon oxides; its specific activity and selectivity are highly support- dependent. For a given cobalt support system both initial and steady state activities were found to increase with increasing loading and decreasing dispersion (4, 31) Selectivity to C_{2+} also increased with decreasing dispersion (4). The extent of Co reduction also played an important role in the activity, increasing with the increase of such parameters (4).

In the Co monometallic sample, due to the reduction temperature employed (623 K) the metal reduced was that coming from the supported oxide, a fact confirmed by its catalytic behavior. In effect, low loading of metallic cobalt highly dispersed in the mordenite showed low specific activities (Table 3) and high selectivity to CH_4 (Fig. 4, Table 4). PtM presented a low specific activity, the CO_2 turnover frequency being of the same order of magnitude as that reported for the Pt/Al_2O_3 system (32). However, the turnover frequency of CH_4 formation for the sample with 5% Pt results in one order of magnitude higher than that of the catalyst. Solymosi and Erdöhelyi (32) reported for 5% Pt/Al_2O_3 a turnover frequency (N = molecules formed or reacted/metal sites · s) of $N_{CO_2} = 0.021\ s^{-1}$ and $N_{CH_4} = 0.002\ s^{-1}$ at 548 K for $H_2/CO_2 = 4:1$ and activation energy of CH_4 formation of 17.5 Kcal/mol. The turnover frequency of CO_2 disappearance was almost independent of the Pt loading in the monometallic samples when dispersion was constant; however, the selectivity to CH_4 strongly increased from samples with low loading (0.5 and 1% Pt) to samples with high loadings (Table 4 and Fig. 4). In order to attempt an explanation of this behavior the reaction mechanism proposed for the hydrogenation of CO_2 in group VIII metals has to be considered. It is generally accepted (33–35) that the reaction occurs mainly through the formation of chemisorbed carbon monoxide (formate species as co-precursors have also been suggested). In a second step the adsorbed CO is dissociated and then the carbon species formed react with the surface hydrogen to form hydrocarbons. From the results obtained, in comparative studies of CO_2 and CO hydrogenation on group VIII metals, several authors concluded that the conversion of CO_2 to CO is a fast step which should not limit the rate of hydrogenation (33, 34). This conclusion could also be valid for alumina-supported Pt according to the results reported by Solymosi and Erdöhelyi (32). Besides, in their study of CO_2 hydrogenation on supported palladium catalysts, Erdöhelyi *et al*. (33) suggested that the carbon formed in the dissociation of CO_2 is easily hydrogenated; this was further demonstrated by Zhang *et al*. (34) using transient kinetic studies over Rh/TiO_2 catalysts. From what is said above, in the mechanism described, the rate of methanation would be determined by the slow step of CO dissociation.

It has been demonstrated that over supported Pd and Rh catalysts (33, 34) the presence of hydrogen enhances the CO dissociation rate due to the formation of a metal-carbonyl hydride intermediate. In such scheme, the ratio of hydrogen and CO coverage of the working catalyst surface must play an important role in the selectivity to CH_4; a high concentration of adsorbed CO could act as surface poison for hydrogen adsorption. This ratio would be affected by the density of the active sites.

The three Pt monometallic samples used in this study have the same dispersion. However, their sites densities (sites density = dispersion × Pt loading)/surface area) are different. It is much higher in the sample with 5% of Pt, which means that the Pt sites are closer than in samples with a low Pt loading. Such proximity of the active sites would improve the interaction between the CO adsorbed and the hydrogen atoms formed and, in this way, enhance the carbon adsorbed species formation. Thus, the selectivity to CH_4 of the samples with high Pt loading is consequently increased.

The results obtained with the bimetallic samples confirm the different characteristics of the species formed after the reduction of the samples at 623 K. The sample with lower Pt content, $Co_{2.0}Pt_{0.5}M$, is the one presenting the highest selectivity to CH_4, compared to the other bimetallic samples. This could be attributed to the metallic Co particles finely dispersed in the main channels of the mordenite. Despite the lower Pt°/Co° ratios, after reduction at 623 K (Table 2), the increase in the specific activity of the bimetallic sample compared to the monometallic one could be attributed to a possible synergetic effect of the Pt particles in intimate contact with those of cobalt. In addition to the promoted action of the Pt in the hydrogen dissociation, this effect could also be understood in terms of the reaction scheme suggested by Somorjai and co-workers (36) for Co foil. Such a proposal is similar to the one previously described (vide supra) but, instead of being hydrogen assisted, the dissociation of surface CO takes place with the formation of CoO. The following reduction of this oxide is the rate limiting step. In this picture, the Pt particles could increase the reducibility of cobalt and enhance the removal of surface oxygen. Similar ideas were suggested by Iglesia *et al*. (37) for Co/TiO_2 catalysts doped with Ru.

In the bimetallic samples with 1% of Pt, where Pt°/Co° is higher than 1 (Table 2, Fig. 2b, reduction temperature $\preceq$623 K) the above effect is more evident, the specific activity of

those samples being almost one order of magnitude higher than the samples with lower Pt content (Table 4).

The selectivity to CH_4 of these samples is lower than that of $Co_{2.0}Pt_{0.5}M$, which could be due to a surface enrichment of Pt in the bimetallic species formed. This effect is stressed in the sample with high Pt content, where the selectivity to methane practically drops to zero (Fig. 4). This behavior was totally different from the Pt monometallic samples with the same loading (Table 4, Fig. 4). These results support those suggested by TPR and XPS and confirmed by DRX, after the sintering process in H_2 stream at 773 K (Fig. 3e) with respect to the formation of bimetallic particles of the $CoPt_3$ type. In fact, in their study of CO chemisorption on the [111] and [100] oriented single crystal surface of the alloy $CoPt_3$, Bardi *et al*. (30) reported that the surface of such bimetallic particles has a pure Pt monolayer. They also suggested that the intermetallic bonding between Co in the second layer and Pt in the top layer changes the electronic state available for the bonding of carbon monoxide. This effect reduces the CO-Pt bond energy and, consequently, the CO formed after CO_2, dissociation in the $CO_2 + H_2$ reaction might not be further dissociated to carbon species. Instead, it could more easily be desorbed and reach the gas phase. In this way, the $CoPt_3$ particles, probably located inside the mordenite main channel, result an active catalyst for the reverse water shift reaction. In fact, from the data in Table 5, it can be concluded that over the $Co_{0.8}Pt_{5.0}M$ the thermodynamic equilibrium composition was reached. Pt monometallic and Pt-Co bimetallic samples also show some activity for the reverse water shift reaction. In fact, the CO concentration in the reactor outlet is higher than the one which corresponds to the simultaneous thermodynamic equilibrium as shown in Table 5.

The results obtained in the $CO_2 + H_2$ reaction at a pressure of 1 atm suggest an interesting behavior of the bimetallic samples, which should be explored at higher pressures to confirm the possible formation of oxygenated compounds.

5. CONCLUSIONS

The present study allows us to stress certain important aspects of the metal-mordenite behavior:

— Co exchanged in NaMordenite presented a very low reducibility in the temperature range under study (273 and 823 K). The Co^{2+} cations were distributed in the mordenite at sites with different stability, suggesting the following order of population: $S_I > S_{VI} > S_{III}$ (Fig. 1a, Table 2).

— Platinum was exchanged in Na mordenite as Pt^{2+} occupying sites of different stability which were reduced in two well-defined temperature zones, 70% in the 273/573 K range and 30% in the 573/823 K range (Figs. 1c, d, e and Table 2). This distribution was independent of the platinum loading.

— The particle size of metallic Pt formed after reduction at 623 K was smaller than 20 Å but after reduction at 823 K it was larger than 30 Å and smaller than 50 Å.

— The incorporation of Pt notably increased the reducibility of Co in the bimetallic mordenite. The type and stability of the species formed after reduction were functions of the Co/Pt ratio (Table 2, Fig. 2).

— Pt mordenite with high Pt loading showed the higher selectivity to CH_4 (Fig. 4). The high site density per surface unit could be responsible for such behavior.

— The promoting effect of Pt had two contributions: on the one hand, a catalytic action activating H_2; on the other, the formation of species of the $PtCo_xO_y$ type as those suggested for other bimetallic systems in zeolites (11–13). Each contribution also depended on the Co/Pt ratio. When this decreased, the catalytic contribution was lower. (Fig. 2, Table 2).

— The Co/Pt interaction in the reduced samples modified the catalytic behavior of monometallic samples in the CO_2 hydrogenation reaction (Table 4, Fig. 4).

— The specific activity and selectivity to CH_4 were also functions of the Co/Pt ratio, thus yielding a catalyst with the maximum methanating activity (maximum turnover frequency of CH_4 formation) for Co/Pt = 0.6.

ACKNOWLEDGMENTS

Financial support was provided by Consejo Nacional de Investigaciones Científicas y Técnicas (CONICET). Thanks are also given to the Japan International Cooperation Agency (JICA) for the donation of the ESCA spectrometer and X-ray diffractometer and to E. Grimaldi for her help in editing the English manuscript.

REFERENCES

1. Mills, G. A., and Steffgren, F. W., *Catal. Rev.* **8**(2), 159 (1973).
2. Bessell, S., *Appl. Catal. A: General* **96**, 253 (1993).
3. Udaya, V., Rao, S., and Gormley, R. J., *Catal. Today* **6**(3), 207 (1990).
4. Bartholomew, C. H., "Studies in Surf. Sci. and Catal." (L. Guczi, Ed.), Vol. 64, p. 158, Elsevier, Amsterdam, 1991.
5. Huang, Y. Y., and Anderson, J. R., *J. Catal.* **40**, 143 (1975).
6. Petunchi, J. O., and Hall, W. K., *J. Catal.* **78**, 327 (1982).
7. Kim, J. C., and Wood, S. I., *Appl. Catal.* **39**, 107 (1988).
8. Zhang, Z., Sachtler, W. M. H., and Suib, S. L., *Catal. Lett.* **2**, 395 (1989).
9. Lu, G., Hoffer, T., and Guczi, L., *Catal. Lett.* **14**, 207 (1992).
10. Sachtler, W. M. H., and Zhang, Z., *Adv. Catal.* **39**, 129 (1993).
11. Lu, G., Zsoldos, Z., Koppány, Z., and Guczi, L., *Catal. Lett.* **24**, 15 (1994).
12. Zsoldos, Z., Vass, G., Lu, G., and Guczi, L., *AppI. Surf. Sci.* **78**, 467 (1994).
13. Guczi, L., Sarkany, A., and Koppány, Z., *Appl. Catal. A: General* **120**, L1 (1994).
14. Lerner, B. A., Carvill, B. T., and Sachtler, W. M. H., *J. Mol. Catal.* **77**, 99 (1992).
15. Lei, G. D., and Sachtler, W. M. H., *J. Catal.* **140**, 601 (1993).
16. Zholobenko, V. L., Lei, G. D., Carvill, B. T., Lerner, B. A., and Sachtler, W. M. H., *J. Chem. Soc. Faraday Trans.* **90**(1), 233 (1994).
17. Li, Y., and Armor, J. N., *Appl. Catal. B: Environmental* **2**, 239 (1993).
18. Gallezot, P., Alarcón-Díaz, A., Dalmon, J-A, Renouprez, A. J., and Imelik, B., *J. Catal.* **39**, 334 (1975).

19. "Powder Diffraction File," JCPDS, (International Center for Diffraction Data, Swarthmore, PA, 1991.
20. Stencel, J. M., Rao, V. U. S., Diehl, J. R., Rhee, K. H., Dhere, A. G., and De Angelis, R. J., *J. Catal.* **84**, 109 (1983).
21. Andersson, S. L. T. and Howe, R. F., *J. Phys. Chem.* **93**, 4913 (1989).
22. Vedrine, J. C., Dufaux, M., Naccache, C., and Imelik, B., *J. Chem. Soc. Faraday I* **74**, 440 (1978).
23. Arnoldy, P., and Moulijn, J. A., *J. Catal.* **93**, 38 (1985).
24. Brown, R., Cooper, M. E., and Whan, D. A., *Appl. Catal.* **3**, 177 (1982).
25. Schoonheydt, R. A., Vandamme, L. J., Jacob, P. A., and Vyherhoeven, J. B., *J. Catal.* **43**, 292 (1976).
26. Mortier, W. J., *J. Phys. Chem.* **81**(13), 1334 (1977).
27. Ostgard, D., Kustou, L., Poeppelmeier, K. F., and Sachtler, W. M. H., *J. Catal.* **133**, 342 (1992).
28. Park, S., Tzou, M. S., and Sachtler, W. M. H., *Appl. Catal.* **24**, 85 (1986).
29. Mc Cabe, R. W., Wong, C., and Woo, H. S., *J. Catal.* **114**, 354 (1988).
30. Bardi, U., Beard, B. C., and Ross, P. N., *J. Catal.* **124**, 22 (1990).
31. Weatherbee, G. D., and Bartholomew, C. H., *J. Catal.* **87**, 352 (1984).
32. Solymosi, F., and Erdöhelyi, A., *J. Mol. Catal.* **8**, 471 (1980).
33. Erdöhelyi, A., Paztor, M., and Solymosi, *J. Catal.* **98**, 166 (1986).
34. Zhang, Z., Kladi, A., and Verykios, X., *J. Catal.* **156**, 37 (1995).
35. Solymosi, F., Erdöhelyi, A., and Bánsági, T., *J. Catal.* **68**, 371 (1981).
36. Lahtinen, J., Anraku, T., and Somorjai, G. A., *Catal. Lett.* **25**, 241 (1994).
37. Iglesia, E., Soled, S. L., Fiato, R. A., and Vía, G. H., *J. Catal.* **143**, 345 (1993).